Self-Pumping Membraneless Miniature Fuel Cell With an Air-Breathing Cathode

Janet I. Hur, Dennis Desheng Meng, and Chang-Jin "CJ" Kim

***Abstract*—We introduce a simple and compact fuel-cell architecture consisting of only solid channels and demonstrate its validity by developing a miniature direct formic acid fuel cell (DFAFC). The proposed architecture generates electric power while pumping the fuel and removing byproduct CO_2 without any discrete pump, gas separator, or membrane electrode assembly (MEA). The fuel pump and gas separator are embedded in the channel, as reported before, by directionally growing and venting CO_2 byproduct bubbles formed inside the reaction microchannels using "virtual check valve" and microporous hydrophobic venting membrane. The new architecture further eliminates the MEA, along with the issues associated with it, by flowing one stream of fuel and electrolyte mixture in a single channel consisting of both an anode and an air-breathing cathode. The reported system obtains a supply of oxygen directly from quiescent air through a gas-diffusion cathode rather than using an oxygen tank. By eliminating all the ancillary parts, the so-called "packaging penalty," which has been hindering the miniaturization of fuel cells below the order of a centimeter, is avoided. This simple and self-standing fuel-cell unit produces 16.7 mW/cm^2, a performance comparable to the existing bulkier DFAFCs that use external pumps, pressurized oxygen or MEA. [2011-0088]**

***Index Terms*—Bubble pumping, fuel-tolerant, membraneless, micro fuel cells, self-pumping.**

I. Introduction

DESPITE THE needs identified in the field of microelectromechanical systems (MEMS) and considerable development efforts over a decade, miniature power sources below a few millimeters have yet to offer satisfactory performance for practical applications, such as laptops, cell phones, or global positioning systems. While fuel cells are attractive due to the high energy density of its fuels (4900 Wh/L in methanol, 2104 Wh/L in formic acid), they face a few important challenges (e.g., packaging penalty, fuel crossover, fuel delivery, water management, and byproduct removal) to contend as viable candidates for micropower sources.

Manuscript received March 25, 2011; revised September 14, 2011; accepted October 25, 2011. Date of publication December 29, 2011; date of current version April 4, 2012. This work was supported by NSF Award 0824269. The work of J. I. Hur was supported by NSF IGERT: Materials Creation Training Program (MCTP)-DGE-0654431 and by the California NanoSystems Institute. Subject Editor Y. Zohar.

J. I. Hur and C.-J. Kim are with the Mechanical and Aerospace Engineering Department, University of California at Los Angeles, Los Angeles, CA 90095-1597 USA (email: janethur@ucla.edu; cjkim@seas.ucla.edu).

D. D. Meng is with the Mechanical Engineering-Engineering Mechanics Department, Michigan Technological University, Houghton, MI 49931, USA (e-mail: dmeng@mtu.edu).

Color versions of one or more of the figures in this paper are available online at http://ieeexplore.ieee.org.

Digital Object Identifier 10.1109/JMEMS.2011.2176920

One of the main challenges in miniaturizing fuel cells to below a centimeter has been the need of ancillary parts such as a fuel pump and a gas separator to build a complete fuel-cell system. Since these parts, particularly the pump, cannot be easily scaled down, they take up increasingly more volume relative to the fuel in a miniaturized system—a critical issue known as the "packaging penalty." To overcome this issue, our group [1], [2] has previously introduced a self-circulating fuel cell, eliminating the ancillary parts—liquid pump for fuel delivery and phase separator for CO_2 bubble removal. The key innovation was the combination of embedded bubble pumping and gas venting mechanisms in the anodic microchannel. Without any discrete pump, the fuel was nevertheless actively pumped and circulated, maintaining the fuel concentration. In contrast, passive fuel cells rely on fuel diffusion to the electrode, with the inevitable tendency to develop a depletion zone over time [3]–[5].

While the self-pumping mechanism dramatically simplified the anode side as described above, the oxygen source for the cathode side still remains as a bulky attachment in the form of a pressurized oxygen tank, a fan, or microchannels filled with actively pumped, oxygen-saturated electrolyte solution. An air-breathing cathode is acceptable for some cases of both direct methanol fuel cell (DMFC) [5]–[7] and direct formic acid fuel cell (DFAFC) [3], [8], [9]. Oxygen from ambient air is readily supplied to the air-breathing cathode, which is practical if the system allows enough free convection of air. However, the performance of the whole system may seriously suffer if the oxygen supply is hindered by water flooding or limited area open to air, particularly when high current density is drawn [10], [11]. Although an air-breathing cathode bears problems stated above, when designed carefully, it is an attractive method to replace the bulky oxygen tank.

Aiming to provide a systematic solution for microfuel cells with the self-pumping mechanism, we focused on the elimination of the membrane electrode assembly (MEA), which has been regarded as an essential component of most low-temperature fuel cells. However, the two-compartment configuration, separated by an MEA, is closely associated with many problems of fuel-cell systems, including fuel crossover, cathode flooding, anode drying out, and difficulty in miniaturization and integration with MEMS [12]. Recently, microfluidic membraneless fuel cells have been developed that flow two laminar streams of fuel and oxidant side by side to establish a virtual proton exchange membrane, thus eliminating the physical MEA and significantly reducing the above-discussed problems [9], [13]–[19]. Alternatively, the MEA can be eliminated from a fuel-cell system by flowing a mixed reactant into reaction

site consisted of selective catalysts [20]–[25], for which case the design of fuel cell is extremely simplified. While these methods eliminate the need of an MEA, an external pump is still necessary to deliver the fuel into the reaction channel. Laminar-flow-based fuel cells particularly need active fuel pumping with certain flow rates to maintain the laminar interface between the fuel and oxidant streams [26].

In this paper,we report an active fuel cell that uses neither an MEA nor ancillary parts by implementing the self-pumping mechanism into the membraneless design for their synergic advantages. The concept of this new architecture is proven by successfully demonstrating a self-standing miniature fuel cell and confirming its power-generating capability, expanded from our report at a technical conference [27]. Consisting of only solid-state structures with no moving parts, the simple system not only helps constructing miniature fuel cells but also shows a potential for scalable design and manufacturing, which may lead to regular-scale systems as well.

II. Mechanism

By embedding the bubble-driven micropumping mechanism [28] into fuel-cell microchannels, Meng and Kim [1] utilized the CO_2 bubbles formed inside the reaction microchannels to pump the fuel. An abrupt change in the inner diameter of the channel, called a "virtual check valve," was placed at the entrance of the channel to block the bubble from growing toward the fuel inlet, and thus directed the bubble to grow only toward the outlet. After expanding to reach the nanoporous hydrophobic venting membrane, the CO_2 was removed through the numerous pores in the venting membrane [2], completing one pumping pulse and starting the next. The result was a directional pumping and circulation of the fuel, as confirmed with an MEA-based micro DMFC [1].

Since the bubble pumping action tends to disrupt the flows and mix the fluid inside the channel, instead of employing laminar-flow-based fuel cell, we considered flowing a single stream of premixed fuel and electrolyte as a better platform to design membraneless self-pumping fuel cells. Unlike other mixed-reactant fuel cells where fuel and oxidant are mixed, oxygen is supplied through an air-breathing cathode to the catalyst-electrolyte interface in order to eliminate oxygen deficiency as a factor in developing the new architecture. Generally, when flowing a mixed stream, the anode and cathode catalysts should selectively oxidize the fuel and reduce the oxygen, respectively. Platinum is known to be one of the preferred catalysts for both fuel oxidation and oxygen reduction. However, platinum has not been considered as a preferable catalyst for the cathode of mixed-reactant fuel cells due to the severe mixed potential. As a result, other fuel-tolerant materials with inferior catalytic activities (e.g., non-noble metals) are commonly used as the cathode catalysts. Interestingly, however, we have found that the platinum is fuel tolerant in our design, allowing us to use platinum for the cathode catalyst. This unexpected but welcome discovery is discussed later in the *Results and Discussion* section. While Pt is used as the catalyst on the cathode, Pd on the anode provides an initial selectivity in the mixed reactant situation. Pd is also a better catalyst in DFAFC [29].

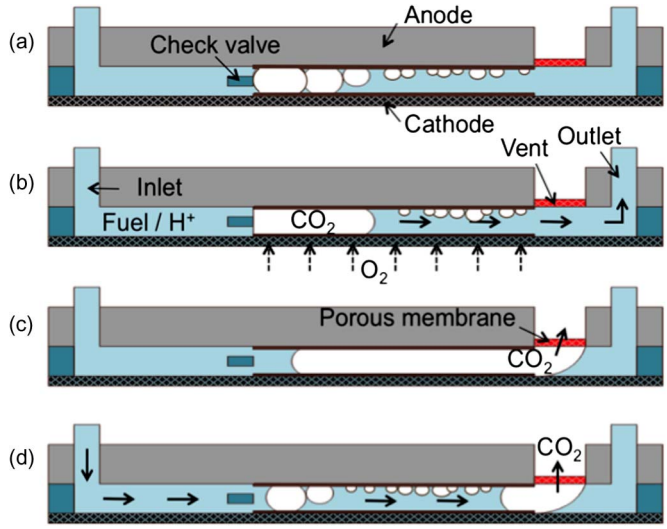

Fig. 1. Schematic illustration of bubble pumping mechanism for the proposed self-pumping membraneless fuel cell, shown from the side of the device. (a) A mixed stream of fuel and electrolyte starts the reaction on each electrode, creating CO_2 bubbles inside the channel. (b) As the bubbles grow, they merge into a single large bubble. Further growth of the bubble is blocked by the check valve near the inlet forcing the bubble to propagate to the right inside the reaction channel. This process pushes the used fuel stream out to the outlet. (c) When the bubble grows long enough to reach the porous membrane, only gas vents through the membrane. (d) As the bubble shrinks due to the venting, fresh fuel is streamed into the channel, starting the next pumping cycle.

The schematic illustration in Fig. 1 describes the working mechanism of a membraneless self-pumping fuel cell proposed and developed in this paper. First, the reactant channel is filled with a fuel–electrolyte mixture. When the two fuel-cell electrodes (anode and cathode) are connected through an electrical load, the electrocatalytic reaction starts to generate power, producing CO_2 as a byproduct. The CO_2 nucleates on the anode catalyst as bubbles start to grow, as shown in Fig. 1(a). Soon the bubbles merge into a large bubble, which grows rightward because the virtual check valve blocks the leftward growth, pushing the liquid toward the outlet, as shown in Fig. 1(b). During the process, the large bubble collects and clears most of the bubbles in the reaction channel. After growing to reach the venting membrane, as described in Fig. 1(c), the bubble is removed rapidly through the hydrophobic nanoporous membrane. While the bubble shrinks (by venting), fresh fuel is pulled in, starting a new cycle of reaction and pumping, as shown in Fig. 1(d). Because the bubble starts to appear first near the check valve, the size of the bubble is larger on the left inside the reaction channel within a pumping cycle. The bubble right next to the check valve is always the largest, minimizing the backflow and keeping the self-pumping mechanism inherently efficient.

III. Device Fabrication

Fig. 2 shows the device we developed to test the concept of mixed-reactant self-pumping fuel cell. Anode was made of 5 mm thick graphite plate (EDM Supplies Inc.) cut into 75 mm in length and 20 mm in width. Three holes of 5 mm in diameter were drilled to form inlet, outlet, and gas vent. After the machining is done, the graphite plate is rinsed with methanol and sonicated in a water bath to remove the debris and particles

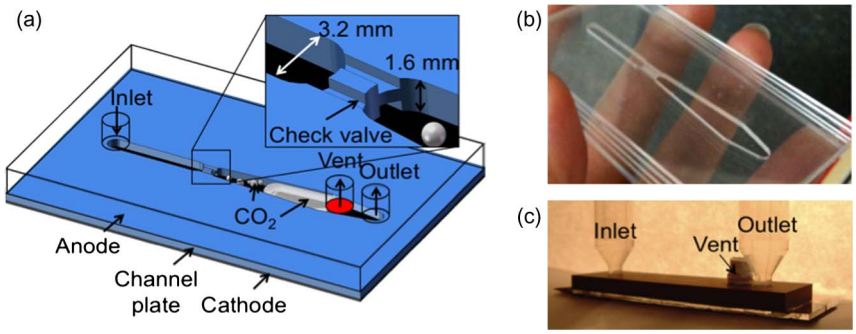

Fig. 2. Fabrication of the self-pumping membraneless fuel-cell test device. (a) Schematic showing three parts: anode, channel plate, and cathode. The graphite anode, drawn transparent, has three drilled holes for liquid inlet, outlet, and gas vent. The channel plate, CNC-machined out of a PMMA and drawn in bright blue, defines the microchannel shape and provides the virtual check valve. The thin dark blue plate on the bottom is an air-breathing cathode. (b) The fabricated transparent channel plate, and (c) the final assembled device with reservoirs used for visualizing fuel delivery.

generated during the machining. A Pd catalyst ink was dropped and dried to cover the reaction area, loading 2 mg/cm^2 of Pd black on the graphite plate. A channel plate was made by cutting the channel shape out from a 1.6 mm thick clear PMMA sheet using the Prolight CNC milling machine. A check valve was designed into the channel (see the magnified figure in the inset) to block the bubble growth. The channel was configured in a diverging shape so that the built-in pressure difference between the left and right meniscus of the bubbles in the channel helps the medium-size bubbles move toward the outlet even before the large bubble is formed and directed by the check valve. The sidewalls of the channel were made transparent by polishing the surface with grade 1500 sandpaper and a polishing compound (Turtle Wax) to allow visual observation of the bubble pumping process during experiments. In the device demonstrated here, cathode was made of a carbon cloth with 0.5 mg/cm^2 using 30 wt% Pt on Vulcan XC-72. A Pt catalyst ink was dropped and dried, loading 2 mg/cm^2 of additional Pt black on the reaction area. The prepared carbon cloth served as air-breathing cathode to use a high oxygen supply from the ambient air rather than relying on the oxygen dissolved in the fuel-oxidant mixture in conventional mixed-reactant fuel cells.

Catalyst ink was prepared by measuring out a proper amount of Pd black or Pt black particles and adding 10 wt% Nafion solution (Dupont) for proton conduction and particle binding. For each case, deionized water was added to make the total volume 500 μL. Then, we metered a droplet volume to deposit 2 mg of Pd and 1 mg of Nafion per square centimeter for the anode catalyst ink or 2 mg of Pt and 0.1 mg of Nafion per square centimeter for the cathode catalyst ink. After dropping and spreading the catalyst ink on the corresponding electrode, the solvent was evaporated under room temperature. Loading of Pd or Pt black was determined to be 2 mg/cm^2 to prevent the catalyst layer from building internal stress and peel off from the electrode. When ready, the anode and the channel plate were glued with rubber cement and the channel plate and the cathode with epoxy to assemble the device. Rubber cement allowed us to disassemble the anode for modifications, while epoxy provided a strong bonding for the flexible cathode against leaking. Both rubber cement and epoxy are not directly exposed to the fuel stream unless the contamination from smeared electrolyte in the gap in the assembled device diffuses out to the main stream. So far, there has been no noticeable degradation after testing. We used a polytetrafluoroethylene (PTFE) tape, commonly known as "Teflon tape," which is widely available as a sealing material. Compared with the PTFE membrane from Millipore used in preceding work [2], the Teflon tape has a similar pore diameter as seen in Fig. 3(a) and (b). When used in our fuel cell, it properly vented out the CO_2 bubble without leakage. When plugging the venting hole, Teflon tape can seal around the hole without any other sealant.

IV. Experiment

The reported membraneless self-pumping fuel cell developed above has been characterized with a potentiostat/galvanostat Model 263 A (Princeton Applied Research). Our presented data is normalized with respect to the cathodic catalyst-exposed area of 1.0 cm^2, while the area of anode catalyst is smaller (0.78 cm^2) due to the venting hole, to maintain a conservative view. The device was clamped and held in the air for sufficient oxygen supply under room temperature and ambient pressure. The fuel solution was filled into the inlet tubing, and the waste flowed into the outlet tubing. Reservoirs with a large area were connected to inlet and outlet through tubing and placed on the same level to avoid hydraulic pressure build up or gravity-driven fuel delivery during regular fuel-cell testing. To confirm fuel delivery easily, however, reservoirs with a small area were placed above the inlet and outlet [Fig. 2(c)]. One can monitor the fuel delivery simply by reading the levels in the reservoirs. The solution was prepared by mixing various concentrations (0.5M, 1M, 5M, 10M) of formic acid (HCOOH, Sigma-Aldrich) into 1M sulfuric acid (H_2SO_4, EMD), which is fuel and electrolyte, respectively. Here, formic acid was used as the fuel, since more CO_2 bubbles are produced for a given current output, compared with DMFC [30], as shown below.

Direct formic acid fuel cell

$$\begin{aligned} Anode &: \mathrm{HCOOH} \rightarrow \mathrm{CO_2} + 2\mathrm{H^+} + 2e^- \\ Cathode &: \frac{1}{2}\mathrm{O_2} + 2\mathrm{H^+} + 2e^- \rightarrow \mathrm{H_2O}\ . \end{aligned} \tag{1}$$

Direct methanol fuel cell

$$\begin{aligned} Anode &: \mathrm{CH_3OH} + \mathrm{H_2O} \rightarrow \mathrm{CO_2} + 6\mathrm{H^+} + 6e^- \\ Cathode &: \frac{3}{2}\mathrm{O_2} + 6\mathrm{H^+} + 6e^- \rightarrow 3\mathrm{H_2O}. \end{aligned} \tag{2}$$

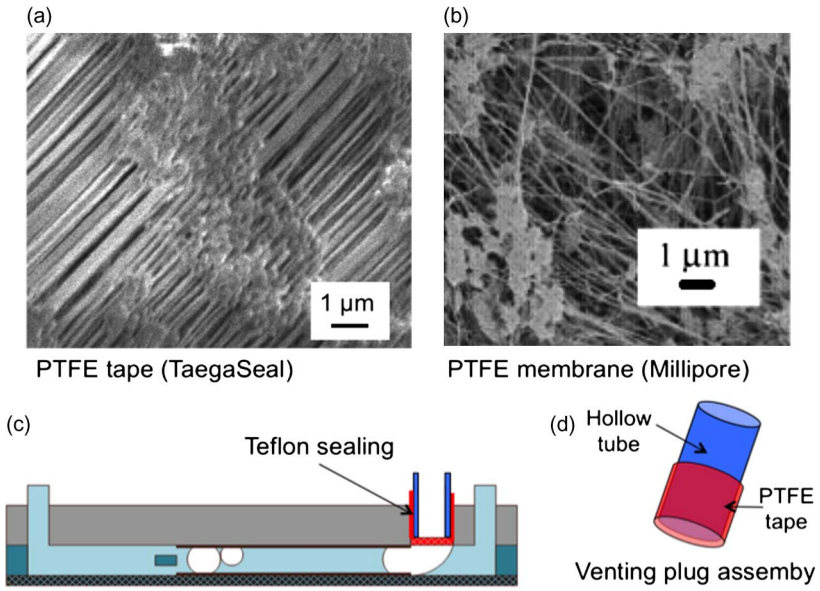

Fig. 3. (a) SEM of PTFE tape (TaegaSeal) and (b) PTFE membrane (Millipore). Although PTFE tape has more directional pore patterns, they both have pore sizes in the order of 100 nm. (c) In the final device, venting plug assembly is plugged into the venting hole. PTFE tape wrapped around a hollow tube gives air-tight sealing, and (d) hollow tube of venting plug assembly gives a structural support to the PTFE venting membrane.

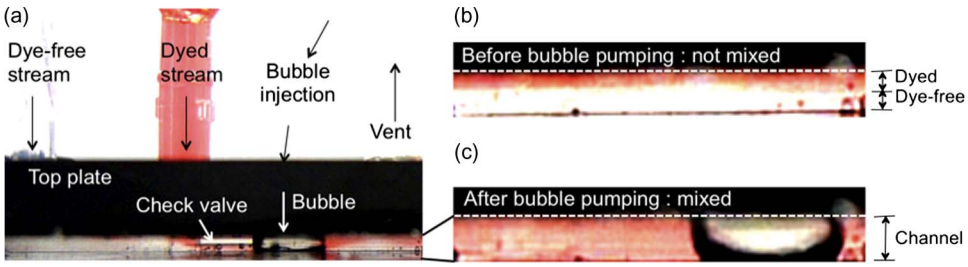

Fig. 4. Feasibility of employing the bubble-pumping mechanism into laminar-flow-based fuel cells was tested using a dyed fuel. (a) After pumping a dyed stream (red) and dye-free stream (clear) through the top plate (shown black) into the microchannel to establish a laminar interface, we injected bubbles with a syringe into the right end of the valve. (b) Before the bubble pumping, the dyed stream flows parallel to the dye-free stream without mixing. (c) After few cycles of bubble pumping, the two streams are found mixed. Please see the colored version for clarity.

Diluted sulfuric acid is used as an electrolyte for proton conduction through the liquid inside the channel. At the same time, it serves as the medium for oxygen to diffuse from ambient air into the vicinity of the cathode. Bubble pumping was recorded with a digital camera from the side of the device through the transparent channel plate.

V. Results and Discussion

A. Bubble Pumping

Before employing the reported architecture to eliminate MEA, we have concluded applying the bubble pumping mechanism to the membraneless microfluidic fuel cell of fuel-oxidant laminar streams is impractical at this point. To evaluate the feasibility, we have tested the effect of moving bubbles, as shown in Fig. 4, by flowing a dyed water stream laminarly in parallel with a dye-free water stream. Then, bubbles were injected into the channel by a syringe to mimic the bubble pumping of the self-pumping fuel cell. After a few cycles of bubble injection and venting, however, the two streams were found to be mixed. Although it may be possible to minimize the disruption of the laminar flows by design optimization eventually, we decided to employ a mixed-reactant fuel-cell approach in our system.

Different from the normal fuel-cell testing conditions, a setup with individual reservoirs above the inlet and outlet was used for an easy visual confirmation of fuel delivery. A successful bubble pumping would deliver the fuel from the inlet to outlet and make the level of the fuel reservoir fall and that of the waste rise. The pumping action inside the channel was visually observed from the side through the transparent channel plate. Some snap shots of the video recordings are presented in Fig. 5, which confirms that the CO_2 bubbles grow directionally to the right toward the venting site [Fig. 5(a) and (b)]. As the large bubble leaves the channel through the venting membrane and a fresh fuel enters the reaction channel from the left, new small bubbles start to nucleate near the entrance [Fig. 5(c) and (d)], starting a new pumping cycle, as designed in Fig. 1. At the same time, we observed that the liquid level of the waste reservoir above the outlet rose and the level of the fuel reservoir above the inlet fell, when bubble reached venting membrane and left the channel. On the other hand, the level in fuel reservoir maintained its level while bubble was growing, confirming that the CO_2 bubbles generated by the fuel-cell electrochemistry indeed pump the fuel mixture across the channel. However,

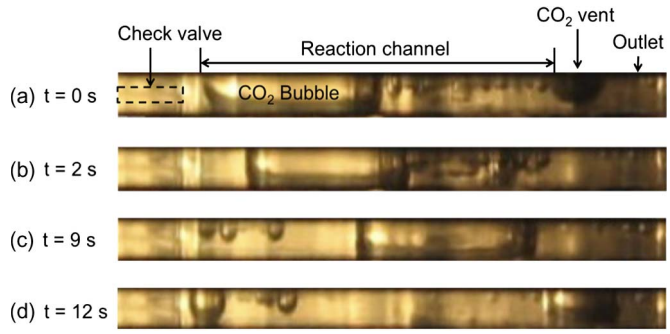

Fig. 5. Snapshots of bubble pumping taken during fuel-cell operation. 1 M formic acid was used as fuel mixed in 1M sulfuric acid under ambient pressure and room temperature. CO_2 bubbles successfully nucleated, grew, merged, moved along the diverging channel, and vented out of the channel through the hydrophobic nanoporous membrane.

the setup in this experiment, designed particularly to prove the concept with a focus on visual confirmation of the self-pumping mechanism, is not capable of operating as a fuel cell for long, because the hydraulic backpressure eventually grows too high to pump against. Although the fuel is delivered by surface tension and in essence not sensitive to gravitational orientation, the device in this experimental setup is affected by the hydraulic pressure; note the fuel column falls and the waste column rises as the fuel is consumed. These columns are made open to air and placed vertical in this experiment to confirm the proposed device can pump against a backpressure. In real practice, a complete fuel-cell system will be designed so that the fuel cartridge is slightly pressurized or balanced with the waste side.

In order to theoretically assess the capability of the reported method to supply enough fuel for the reaction, we estimated the rate at which the microchannel can be refreshed at certain electrical current output. To simplify the analysis, we assume that the large CO_2 bubble fills up the entire reaction channel (between the check valve and the gas vent). The number of CO_2 molecules needed to fill up the channel is estimated using the ideal gas law under standard conditions for temperature and pressure

$$PV = nRT \tag{3}$$

where P is the absolute pressure of the gas, V is the volume of the gas, n is number of moles, R is the universal gas constant, and T is the absolute temperature. Since two electrons need to flow from anode to cathode to produce one molecule of CO_2, it is calculated that the present test device (the geometries given in the *Device fabrication* section) needs to produce a $\sim$20 mA/cm^2 of current density in order to refresh the channel every 1 min. The timescale in this calculation was selected, following the repeatedly observed pumping frequency during experiment. Qualitatively speaking, the production of a higher current will generate CO_2 bubbles faster, resulting in more frequent channel refreshments and a faster flow rate of the fuel. Depending on the current density, which we control through the external electric load connecting the fuel-cell electrodes, the time for one pumping cycle varied from a few tens of seconds to minutes. The frequency of bubble pumping was measured increasing linearly with the current density, as shown in Fig. 6(a). The experimental result of bubble pumping is approximately half of the ideal calculated case (e.g., $\sim$40 mA/cm^2 required for bubble pumping frequency of 1/min). The discrepancy comes from the small bubbles near the venting area, which escape directly through the hydrophobic membrane without contributing to pump and the occasional leakage through the air-breathing cathode rather than the venting membrane. We also quantified the pumping rate by monitoring the volume of bubbles leaving the channel in Fig. 6(b) since the volume of bubbles is not consistent throughout the cycles. Since the diverging channel also assists refreshing the fuel, the frequency cannot give an accurate pumping rate by itself. The results show a linear trend that CO_2 production and pumping are proportional to the amount of current generated. Although the observed frequency of bubbles leaving at 50 mA/cm^2 is lower than that at 40 mA/cm^2 in Fig. 6(a), the measured pumping rate at 50 mA/cm^2 is higher than that at 40 mA/cm^2 in Fig. 6(b). The bubble pumping frequency is somewhat less reliable because the volumes of bubbles involved in pumping are not consistent.

In our next set of experiments, the inlet and outlet shared the same reservoir, eliminating the hydraulic pressure and recirculating the fuel. A longer testing is presented in Fig. 7. The device continued to refresh its channel with new streams of fuel and kept running. In contrast, once the venting site of the same device was blocked for comparison, the current density decreased soon. However, this blocked device maintained higher current densities and decreased slowly compared to Meng and Kim [1]. The discrepancy can be understood by noting some bubbles leak through the air-breathing cathode in the current device. The lost volume of bubbles is filled by the fuel from inlet or outlet, replenishing a small amount of additional fuel to the channel. However, this supply does not have a directional pumping effect. Therefore, over time, the current eventually dies out until there is no significant bubble growth.

B. Air-Breathing Cathode

The cathode can evaporate the excessive water formed within the cathode layer but keeps the bulk liquid inside the cell. Even though we sometimes left the cell to obtain stabilized OCP over hours, meaning no current density but evaporation through the cathode, both electrodes including air-breathing cathode did not show any sign of drying out. We saw small water droplets condensed on the bench surface near the cathode, indicating some evaporation, when running under higher current densities ($\sim$50 mA/cm^2). Without any leakage seen, the cathode keeps the liquid inside the cell. At high pressures (tens of kPa), the fuel can leak through the cathode [2]. However, the proposed cell is not pressurized by any auxiliary components such as liquid pump and brings the fuel into the reaction channel only by surface tension. The Laplace pressure built up by the bubble menisci is on the order of hundreds of Pa, which is safely lower (by two orders of magnitude) than the leakage pressure.

C. Catalytic Activities

In the conventional fuel-cell configuration, Pt is considered as a desirable option for both anode and cathode. However, the

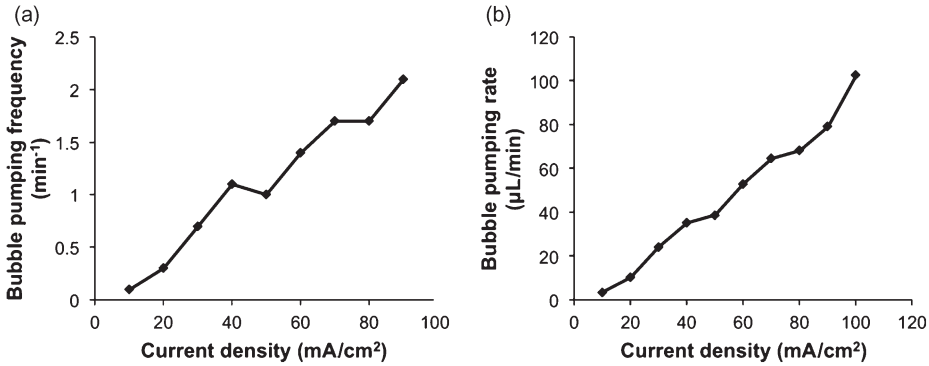

Fig. 6. Pumping frequency and rate of designed fuel cell. (a) Frequency of bubble pumping generally increases with the current density generated. Since the frequency only counts the number of bubbles, it does not directly account for the volume of pumping. (b) Measured with the volume of each bubble leaving the venting site, the bubble pumping rate is found proportional to the current density.

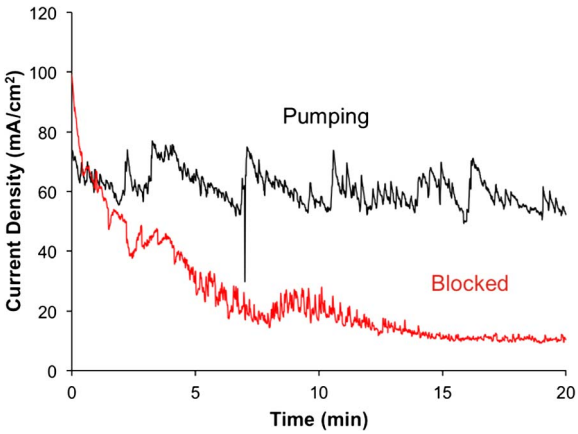

Fig. 7. Comparison of bubble pumping enabled and blocked. During bubble pumping, a current density is maintained, and the device keeps pumping and generating power as long as fuel is available. However, when the venting site is blocked so that the bubble pumping is disabled, current density soon decreased. The experiment was done with fuel inlet and outlet connected to a common reservoir to avoid the hydraulic pressure build up. A mixture of 20 mL of 1 M fuel and 1 M electrolyte was used.

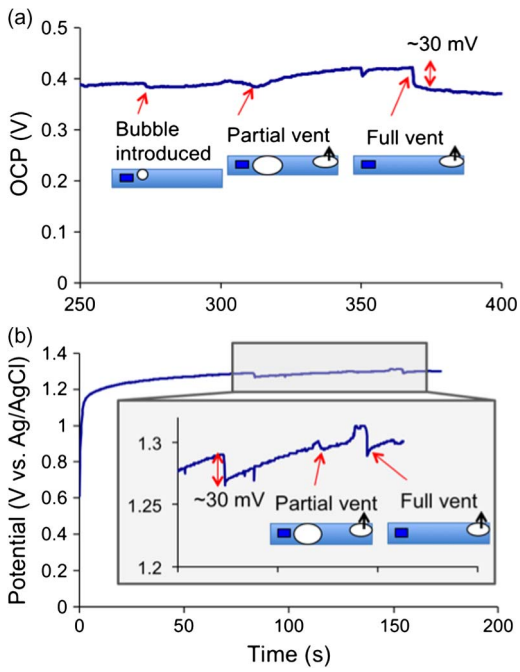

Fig. 8. Effect of bubble pumping, moving, and venting on cathode electrode. (a) The experiment was performed by manually injecting air bubbles to mimic bubble pumping while monitoring the OCP in fuel cell. The maximum observed fluctuation, which corresponded to a large bubble fully venting out and inducing a rapid stream of new fuel into the channel, was only ~30 mV. (b) Potential of the cathode was monitored against the reference electrode (Ag/AgCl) under a constant current of 30 mA/cm^2 to the cell. On the anode, there was bubble forming and pumping similarly to the fuel-cell reaction. Potential fluctuation was ~30 mV, suggesting the bubble action mostly affected the cathode. Both experiments used 2 M formic acid.

mixed potential issue [20], [24] makes it an undesirable choice to simultaneously employ Pt as the catalyst for both anode and cathode in a given mixed-reactant fuel cell. Particularly, the mixed potential issue is severe at the cathode, since Pt is prone to oxidize fuel while it is supposed to reduce oxygen. As a result, a non-noble metal is commonly used as the cathode catalyst. Contrary to this common practice, as mentioned in the *Mechanism* section, we have found an interesting phenomenon that Pt can be used as a fuel-tolerant cathode catalyst in our design. If we focus on the air-breathing cathode, O_2 is directly supplied through the air-breathing cathode from ambient air to electrolyte/catalyst interface where both the fuel (HCOOH) and supporting electrolyte (H_2SO_4) exist. Considering the equilibrium constant of HCOOH ($K_a = 1.8 \times 10^{-4}$) and H_2SO_4 in water ($K = 2.4 \times 10^6$), the number of HCOOH molecules desiring to break and oxidize on the cathode is far less than H^+ ions dissociated from H_2SO_4 ready to join with O_2 from ambient air by ten orders of magnitude. Therefore, the cathode of presented mixed-reactant fuel cell seems to have fuel tolerance.

We have further tested how the bubble pumping would affect the catalytic activities on both electrodes. Fig. 8 indicates that the bubble growing, moving, and venting do not

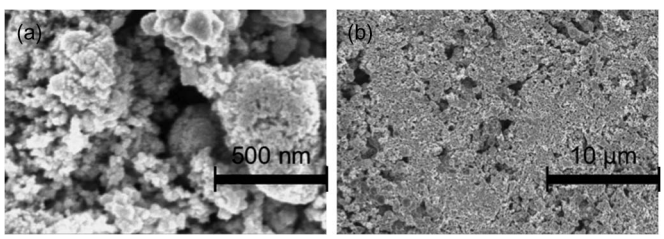

Fig. 9. SEM images of solution-deposited Pd electrocatalyst. (a) At closer view, Pd black has cluster-like structures with nanometer scale roughness. (b) In micrometer scale view, the catalyst layer is rather flat and lacks the hierarchical structure of (a).

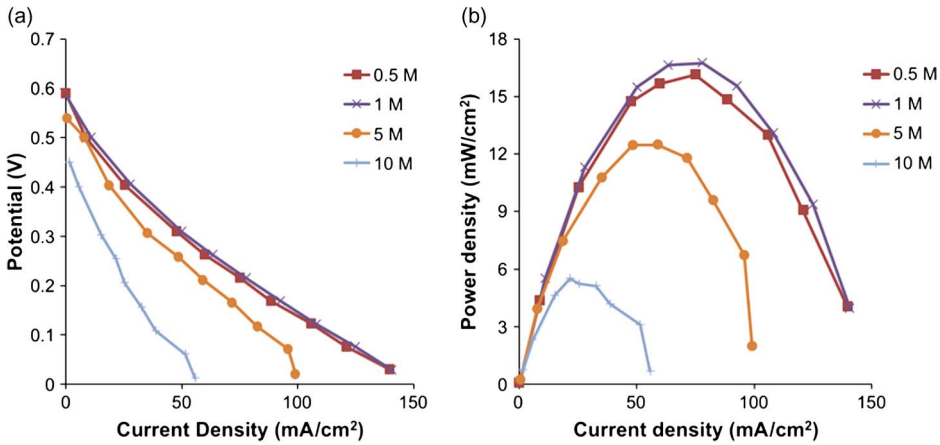

Fig. 10. (a) Polarization and (b) power density curves of the device tested using four different HCOOH concentrations and 1 M H_2SO_4 supporting electrolyte. Polarization curve was taken under room temperature while the fuel cell was bubble pumping. At 0.5 M and 1.0 M of HCOOH, the highest peak power density was seen 16.7 mW/cm^2, which is comparable to or higher than other DFAFCs with quiescent air as the oxygen source. At higher concentration of 5 M and 10 M HCOOH, both OCP and current output dropped.

significantly disturb the potential between the two electrodes. First, in Fig. 8(a), the total disturbance in the fuel cell was monitored by investigating the OCP fluctuation while injecting bubbles through a syringe manually. The greatest disturbance of $\sim$30 mV was seen when the bubble was removed to induce a rapid flow of fresh fuel mixture into the channel. On the other hand, a constant current of 30 mA/cm^2 was supplied to the cell while monitoring the cathode potential (versus Ag/AgCl), and the bubble grew similarly to the fuel-cell reaction. Similar fluctuation behavior of $\sim$30 mV at most is seen in Fig. 8(b). This indicates that the bubble action is disturbing mostly the cathode, which is still only a negligible effect. We also noted that, when the bubble grew to take up the space inside the channel, the potential gradually rose likely because the bubble provided a clear separation between the anode and the cathode.

Surfaces of the deposited catalysts were investigated under scanning electron microscopy (SEM). High surface area is desirable for higher electrocatalytic reaction kinetics on each electrode. Although the highly magnified view [Fig. 9(a)] shows a hierarchical structure in nanometer scale, the Pd black has fairly even and flat surface with little porosity in micrometer scale [Fig. 9(b)], which is not desirable. Compared with the electroplated version [31], the solution-deposited catalyst black used here produced less roughness in micrometer scale, which may not be sufficient to catalyze fuel-cell reactions. Electroplated catalyst black surface is expected to improve the fuel-cell performance in the next-generation devices.

D. Polarization Curve

The polarization and power density curve of the fabricated devices using different HCOOH concentrations and 1 M H_2SO_4 supporting electrolyte has been tested and presented in Fig. 10(a) and (b). Using 1.0 M HCOOH, OCP of 0.59 V and 16.7 mW/cm^2 of peak power density have been obtained, and 0.5 M HCOOH also reached a similar value of 16.1 mW/cm^2. At higher concentration of 5 M and 10 M HCOOH, OCP dropped to 0.54 V and 0.45 V, respectively, and the current density output was decreased due to a mixing issue at the cathode. The OCP in presented device is relatively lower due to its mixed-reactant nature. Compared with other (i.e., fuel flowing by an external pump) DFAFCs utilizing quiescent air as an oxygen source, our measured value is comparable to the $\sim$12 mW/cm^2 of peak power density in [3], which used a silicon fabricated MEA using Pt as the cathode catalyst, and higher than the $\sim$8 mW/cm^2 of peak power density in [22], which used RuSeW as the fuel-tolerant cathode catalyst along with a fuel mixed with air in a vaporizer. Although the current study is to develop and prove the new concept of self-pumping fuel-cell mechanism with a mixed reactant of fuel and electrolyte, we have observed few phenomena that unveil future research directions.

VI. Conclusion

A self-standing membraneless fuel cell of a very simple design has been proposed and realized. With neither ancillary parts nor MEA, we were able to successfully build and test the fuel-cell system consisting only of a fuel-cell assembly, a fuel reservoir, and a waste reservoir. Since we have eliminated the fuel pump, oxygen tank, gas separator, and MEA, all the main issues associated with them have been cleared along with the packaging penalty. By adopting formic acid fuel in our design, the CO_2 bubbles were efficiently generated. However, the choice of fuel and oxygen supply is flexible as long as CO_2 bubbles are produced during electrochemical reaction. Using quiescent air, we have obtained the fuel-cell performance similar to or higher than other reported DFAFCs, which use an external fuel pump, under the same conditions of quiescent air. More studies are in order to understand how Pt works as a fuel-tolerant cathode catalyst in our device relative to other mixed-reactant fuel cells.

Acknowledgment

The authors would like to thank Prof. S. Lee for his helpful discussions and express their appreciation to B. Roizen and A. Lee for the help in manuscript preparation.

REFERENCES

[1] D. D. Meng and C.-J. Kim, "An active micro-direct methanol fuel cell with self-circulation of fuel and built-in removal of CO_2 bubbles," *J. Power Sources*, vol. 194, no. 1, pp. 445–450, Oct. 2009.

[2] D. D. Meng, T. Cubaud, C.-M. Ho, and C.-J. Kim, "A methanol-tolerant gas-venting microchannel for a microdirect methanol fuel cell," *J. Microelectromech. Syst.*, vol. 16, no. 6, pp. 1403–1410, Dec. 2007.

[3] J. Yeom, R. S. Jayashree, C. Rastogi, M. A. Shannon, and P. J. A. Kenis, "Passive direct formic acid microfabricated fuel cells," *J. Power Sources*, vol. 160, no. 2, pp. 1058–1064, Oct. 2006.

[4] J. G. Liu, T. S. Zhao, R. Chen, and C. W. Wong, "The effect of methanol concentration on the performance of a passive DMFC," *Electrochem. Commun.*, vol. 7, no. 3, pp. 288–294, Mar. 2005.

[5] T. Shimizu, T. Momma, M. Mohamedi, T. Osaka, and S. Sarangapani, "Design and fabrication of pumpless small direct methanol fuel cells for portable applications," *J. Power Sources*, vol. 137, no. 2, pp. 277–283, Oct. 2004.

[6] C. Y. Chen and P. Yang, "Performance of an air-breathing direct methanol fuel cell," *J. Power Sources*, vol. 123, no. 1, pp. 37–42, Sep. 2003.

[7] T. Hottinen, M. Mikkola, and P. Lund, "Evaluation of planar free-breathing polymer electrolyte membrane fuel cell design," *J. Power Sources*, vol. 129, no. 1, pp. 68–72, Apr. 2004.

[8] S. Ha, B. Adams, and R. I. Masel, "A miniature air breathing direct formic acid fuel cell," *J. Power Sources*, vol. 128, no. 2, pp. 119–124, Apr. 2004.

[9] R. S. Jayashree, L. Gancs, E. R. Choban, A. Primak, D. Natarajan, L. J. Markoski, and P. J. A. Kenis, "Air-breathing laminar flow-based microfluidic fuel cell," *J. Amer. Chem. Soc.*, vol. 127, no. 48, pp. 16 758–16 759, Dec. 2005.

[10] T. Fabian, J. D. Posener, R. O'Hayre, S.-W. Ch, J. K. Eaton, F. B. Prinz, and J. G. Santiago, "The role of ambient conditions on the performance of a planar, air-breathing hydrogen PEM fuel cell," *J. Power Sources*, vol. 161, no. 1, pp. 168–182, Oct. 2006.

[11] M. Paquin and L. G. Frechette, "Understanding cathod flooding and dry-out for water management in air breathing PEM fuel cells," *J. Power Sources*, vol. 180, no. 1, pp. 440–451, May 2008.

[12] G. Q. Lu, C. Y. Wang, T. J. Yen, and X. Zhang, "Development and characterization of a silicon-based micro direct methanol fuel cell," *Electrochim. Acta*, vol. 49, no. 5, pp. 821–828, Feb. 2004.

[13] K. S. Salloum and J. D. Posner, "A membraneless microfluidic fuel cell," *J. Power Sources*, vol. 196, no. 3, pp. 1229–1234, Feb. 2011.

[14] K. S. Salloum, J. R. Hayes, C. A. Friesen, and J. D. Posener, "Sequential flow membraneless microfluidic fuel cell with porous electrodes," *J. Power Sources*, vol. 180, no. 1, pp. 243–252, May 2008.

[15] J. L. Cohen, D. J. Volpe, D. A. Westly, A. Pechenik, and H. D. Abruna, "A dual electrolyte H2/O2 Planar membraneless microchannel fuel cell system with open circuit potentials in excess of 1.4 V," *Langmuir*, vol. 21, no. 8, pp. 3544–3550, Apr. 2005.

[16] E. R. Choban, L. J. Markoski, A. Wieckowski, and P. J. A. Kenis, "Microfluidic fuel cell based on laminar flow," *J. Power Sources*, vol. 128, no. 1, pp. 54–60, Mar. 2004.

[17] R. Ferringo, A. D. Stroock, T. D. Clark, M. Mayer, and G. M. Whitesides, "Membraneless vanadium redox fuel cell using laminar flow," *J. Amer. Chem. Soc.*, vol. 124, no. 44, pp. 12 930–12 931, Nov. 2002.

[18] E. Kjeang, A. G. Brolo, D. A. Harrington, N. Djilali, and D. Sinton, "Hydrogen peroxide as an oxidant for microfluidic fuel cells," *J. Electochem. Soc.*, vol. 154, no. 12, pp. B1220–B1226, Oct. 2007.

[19] E. Kjeang, R. Michel, D. A. Harrington, D. Sinton, and N. Djilali, "An alkaline microfluidic fuel cell based on formate and hypochlorite bleach," *Electrochim. Acta*, vol. 54, no. 2, pp. 698–705, Dec. 2008.

[20] T. S. Olson, B. Blizanac, B. Piela, J. R. Davey, P. Zelenay, and P. Atanassov, "Electrochemical evaluation of porous non-platinum oxygen reduction catalysts for polymer electrolyte fuel cells," *Fuel Cells*, vol. 9, no. 5, pp. 547–553, Oct. 2009.

[21] A. K. Shukla, R. K. Raman, and K. Scott, "Advances in mixed-reactant fuel cells," *Fuel Cells*, vol. 5, no. 4, pp. 436–447, Dec. 2005.

[22] H. Cheng, W. Yuan, and K. Scott, "A liquid-gas phase mixed-reactant fuel cell with a RuSeW cathode electrocatalyst," *J. Power Sources*, vol. 183, no. 2, pp. 678–681, Sep. 2008.

[23] D. T. Whipple, R. S. Jayashree, D. Egas, N. Alonso-Vante, and P. J. A. Kenis, "Ruthenium cluster-like chalcogenide as a methanol tolerant cathode catalyst in air-breathing laminar flow fuel cells," *Electrochim. Acta*, vol. 54, no. 18, pp. 4384–4388, Jul. 2009.

[24] K. Scott, A. K. Shukla, C. L. Jackson, and W. R. A. Meuleman, "A mixed-reactants solid-polymer electrolyte direct methanol fuel cell," *J. Power Sources*, vol. 126, no. 1/2, pp. 67–75, Feb. 2004.

[25] W. Sung and J.-W. Choi, "A membraneless microscale fuel cell using non-noble catalysts in alkaline solution," *J. Power Sources*, vol. 172, no. 1, pp. 198–208, Oct. 2007.

[26] E. Kjeang, N. Djilali, and D. Sinton, "Microfluidic fuel cells: A review," *J. Power Sources*, vol. 186, no. 2, pp. 353–369, Jan. 2009.

[27] J. I. Hur, D. D. Meng, and C.-J. Kim, "Membranelss micro fuel cell chip enabled by self-pumping of fuel-oxidant mixture," in *Proc. 23rd IEEE Int. Conf. MEMS*, 2010, pp. 168–171.

[28] D. D. Meng and C.-J. Kim, "Micropumping of liquid by directional growth and selective venting of gas bubbles," *Lab Chip*, vol. 8, no. 6, pp. 958–968, Jun. 2008.

[29] Z. Liu, L. Hong, M. P. Tham, T. H. Lim, and H. Jiang, "Nanostructured Pt/C and Pd/C catalysts for direct formic acid fuel cells," *J. Power Sources*, vol. 161, no. 2, pp. 831–835, Oct. 2006.

[30] C. Rice, S. Ha, R. I. Masel, P. Waszczuk, A. Wieckowski, and T. Barnrad, "Direct formic acid fuel cells," *J. Power Sources*, vol. 111, no. 1, pp. 83–89, Sep. 2002.

[31] R. S. Jayashree, J. S. Spendelow, J. Yeom, C. Rastogi, M. A. Shannon, and P. J. A. Kenis, "Characterization and application of electrodeposited Pt, Pt/Pd, and Pd catalyst structures for direct formic acid micro fuel cells," *Electrochim. Acta*, vol. 50, no. 24, pp. 4674–4682, Aug. 2005.

Janet I. Hur received the B.S. degree in mechanical engineering and the M.S. degree from Sogang University, Seoul, Korea, in 2007 and 2009, respectively. She is currently working toward the Ph.D. degree in microelectromechanical systems field in the Department of Mechanical and Aerospace Engineering, University of California at Los Angeles.

Her research interest is in developing miniature power sources such as microbatteries and microfuel cells.

Dennis Desheng Meng received the Ph.D. degree in mechanical engineering from the University of California at Los Angeles in 2005, along with the Outstanding Ph.D. Award.

He is currently an Assistant Professor in the Department of Mechanical Engineering-Engineering Mechanics, Michigan Technological University, Houghton. After he joined Michigan Tech in August 2007, he started the Multi-Scale Energy Systems Laboratory (MuSES Lab) to work on micro- and nanotechnology for energy applications. The ongoing research projects in the MuSES Lab include microfuel cells, microbatteries, microsupercapacitors, production of metal nanoparticles by short-distance sputtering, microfluidic fabrication of self-healing materials, thermal management for power microelectromechanical systems, and biomedical application of superhydrophilic surfaces.

Chang-Jin "CJ" Kim received the B.S. degree from Seoul National University, Seoul, Korea, the M.S. degree from Iowa State University, Ames, and the Ph.D. degree from the University of California, Berkeley, in 1991, all in mechanical engineering.

Since joining the faculty at the University of California at Los Angeles (UCLA) in 1993, he has developed several courses in MEMS and established a MEMS Ph.D. major field in the Mechanical and Aerospace Engineering Department in 1997. Directing the Micro and Nano Manufacturing Laboratory, he is also a founding member of the California NanoSystems Institute at UCLA. His research interests are in MEMS and nanotechnology, including design and fabrication of micro/nanostructures, actuators, and systems, with a focus on the use of surface tension.

Prof. Kim has served on numerous technical committees and panels, including Transducers, the IEEE International Conference on MEMS, and the National Academies Panel on Benchmarking the Research Competitiveness of the U.S. in Mechanical Engineering. He is currently serving on the Editorial Advisory Board for the *IEEJ Transactions on Electrical and Electronic Engineering* and the Editorial Board for the JOURNAL OF MICROELECTROMECHANICAL SYSTEMS. He has also been active in the commercial sector as a board member, scientific advisor, consultant, and founder of start-up companies. A Fellow of ASME, he was the recipient of the Graduate Research Excellence Award from Iowa State University, the 1995 TRW Outstanding Young Teacher Award, the 1997 NSF CAREER Award, the 2002 ALA Achievement Award, and the 2008 Samueli Outstanding Teaching Award.